

Resistivity imaging technique to delineate shallow subsurface cavities associated with old coal working: a numerical study

Prasenjit Das¹ · Priya R. Mohanty¹

Received: 1 April 2015 / Accepted: 27 January 2016 / Published online: 11 April 2016
© Springer-Verlag Berlin Heidelberg 2016

Abstract Subsidence is an environmental hazard due to subsurface cavities associated with abandoned coal workings in the Eastern Indian coalfields. These cavities pose danger to coal mining of deeper coal seams. Most of these subsurface cavities are unapproachable as no mine plans are available. Here, an attempt has been made to detect and possible delineation of air and as well as water filled cavities applying Electrical Resistivity Imaging (ERI) technique using dipole–dipole, pole–dipole and Wenner–Schlumberger arrays. Models are simulated with a reasonable resistivity value of formations considering board and pillar mining environment in multilayer earth. The inverted resistivity section corresponding to water filled cavities without a barrier could be able to detect three cavities for dipole–dipole and Wenner–Schlumberger arrays, whereas pole–dipole array could detect all four cavities. Later on, with inclusion of 1 m coal as a barrier in the model, the dipole–dipole array could be able to bring the signature of cavities, whereas pole–dipole and Wenner–Schlumberger configuration is unable to provide any signature. Similar resistivity responses are noticed for air filled cavities with and without barrier conditions. When all three arrays data are jointly inverted, there is a significant improvement in resistivity response which enables the detection of water filled as well as air filled cavities with and without a barrier.

Keywords Cavity · Electrical resistivity imaging · Joint inversion · Array

Introduction

The detection of subsurface old abandoned cavities is a challenging problem for the ground stabilization in the Eastern Indian coalfields. For exploration and exploitation of coal from deeper coal seams, it is appropriate to identify unknown cavities to avoid accidents such as ground subsidence. Geologically Raniganj coalfield is situated within Damodar Basin in eastern part of India. Its shape is semi elliptical, elongated and extended up to 3000 km² and geographically lies between latitudes 23°03' and 23°51'N and longitudes 86°42' and 87°28'E. Geological formations in Raniganj coalfield are Talchir, Barakar, Barren Measures, Raniganj and Panchet formations. These formations lie over a basement of magnetic gneisses of Precambrian era. Here coal bearing formations are Barakar and Raniganj formations whereas Barren Measures and Panchet formations are lacking of coal seams.

There are several geophysical techniques to detect subsurface cavities based on their physical properties. Electrical resistivity is one such geophysical technique based on conductivity contrast. Usually, high conductivity contrast is observed over water filled cavities which helps in detection. Many researchers have used electrical resistivity technique to interpret subsurface cavities under various geological condition (Logn 1954; Van Nostrand and Cook 1966; Hallof 1966; Zohdy 1969; Zohdy et al. 1973; Singh and Jha 1972; Jain et al. 1973; Stanley et al. 1976; Loke and Barker 1996a; Reynolds 1997; Maillol et al. 1999; Van Schoor 2002; Colella et al. 2004; Dahlin and Zhou 2004; Maillet et al. 2005; Martinez et al. 2009).

✉ Priya R. Mohanty
priyamohanty@hotmail.com

Prasenjit Das
prasenjit191@gmail.com

¹ Department of Applied Geophysics, Indian School of Mines, Dhanbad, India

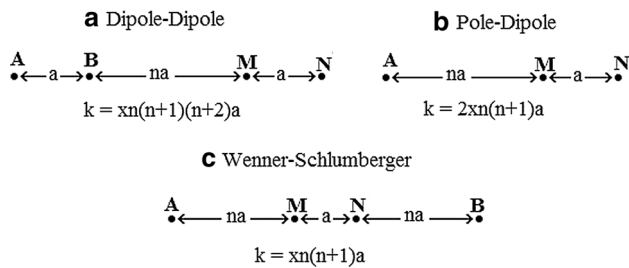


Fig. 1 Geometry of electrode configurations ($x = \pi$, a = dipole length and n = dipole separation factor): **a** dipole–dipole configuration; **b** pole–dipole configuration; **c** Wenner–Schlumberger configuration

Griffiths and Barker (1993), Zhou et al. (2000) and Thomas and Roth (1999) showed a comparison study among twelve methods including four geophysical techniques in the field of sinkhole and subsurface cavity identification. Electrical resistivity tomography survey has been widely used in aquifer researches (Evangelos et al. 2015), environmental and engineering purpose (Chambers et al. 2006; Rucker et al. 2010), hydrogeological (Wilson et al. 2006), mineral exploration (Bauman 2005; Legault et al. 2008) and archaeological (Tsokas et al. 2008). Hutchinson et al. (2002) demonstrated a comparison study among various geophysical methods for void detection. Chalikakis et al. (2011) showed an overview on the contribution of geophysical methods to karst system exploration. Riddle (2012) discussed about all geophysical techniques and their advantages as well as limitations for near surface tunnels and voids detection. Johnson et al. (2002) showed the advantages and disadvantages of all surface geophysical methods for detection of underground mine working. ERI method is used extensively to image the subsurface cavities with greater resolution in shorter time.

Soil gas sampling (^{222}Rn , ^{220}Rn , CO_2) has been used as a technique for abandoned cave detection. Many researchers have identified that radon concentration has been building in coal basin, mine working and in caves (Cigna 2005; Clark 2002; Gillmore et al. 1999; Hakl et al. 1997; Jovanovic 1996; Ntwaeaborwa et al. 2004). Bondarenko et al. (1983) described a radon-mapping technique for detection of the under superficial emptiness. This method defines the streams of radon from soil in border of karstic caves and old galleries.

Combination of different geophysical methods have been used for different geological structures such as: vertical electrical sounding and electrical resistivity tomography (ERT) in saline domain (Zarroca et al. 2011); soil gas sampling (^{222}Rn , ^{220}Rn , CO_2), ERT and seismic refraction profiles in fault zone (Zarroca et al. 2012). This combined approach has been used for subsurface cave

Fig. 2 Inversion results: **a** Resistivity model 1 employed; **b** inverted section using dipole–dipole array; **c** inverted section using pole dipole array; **d** inverted section using Wenner–Schlumberger array; **e** jointly inverted section using dipole–dipole, pole–dipole and Wenner–Schlumberger array

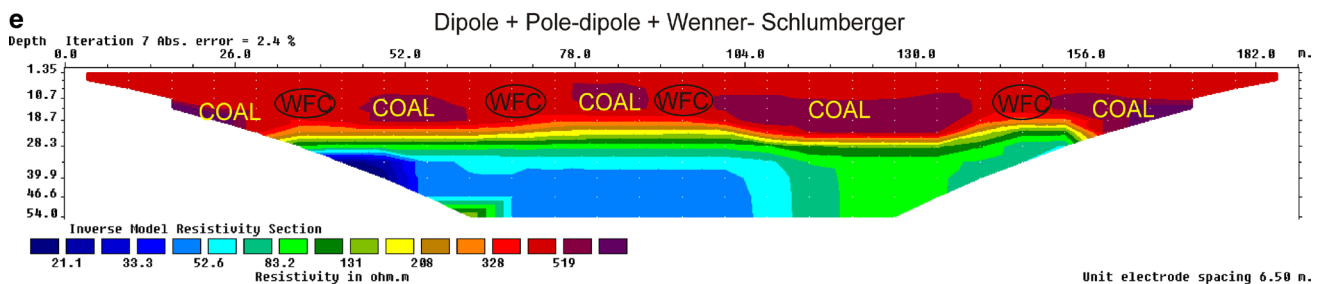
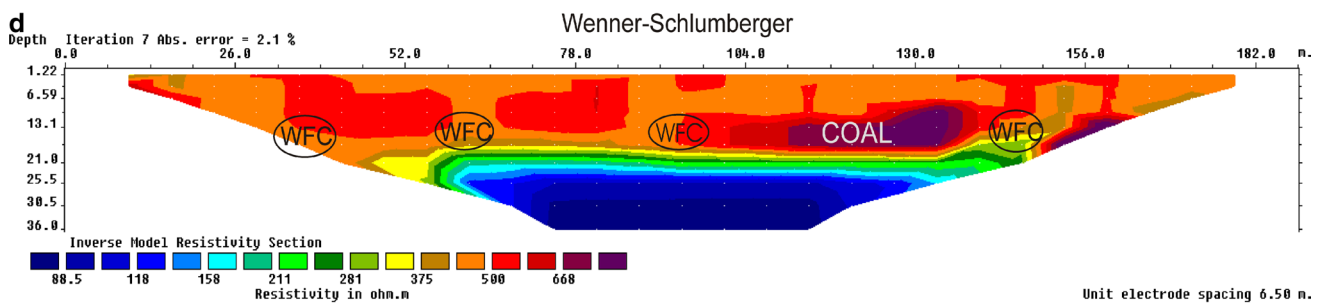
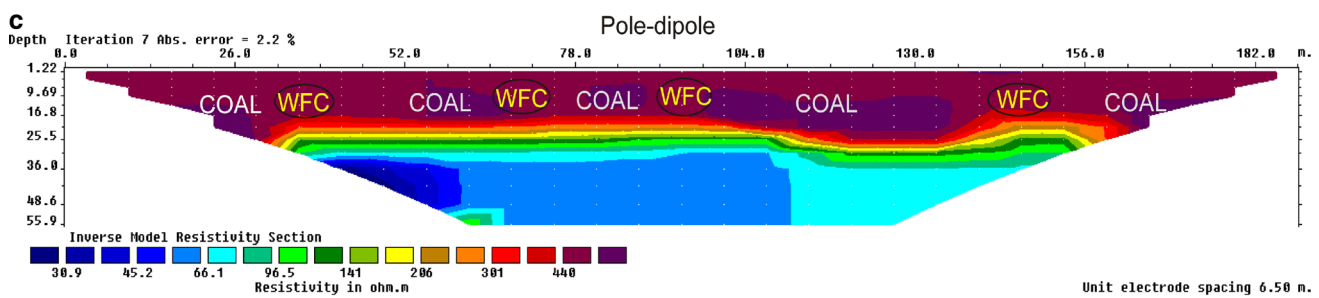
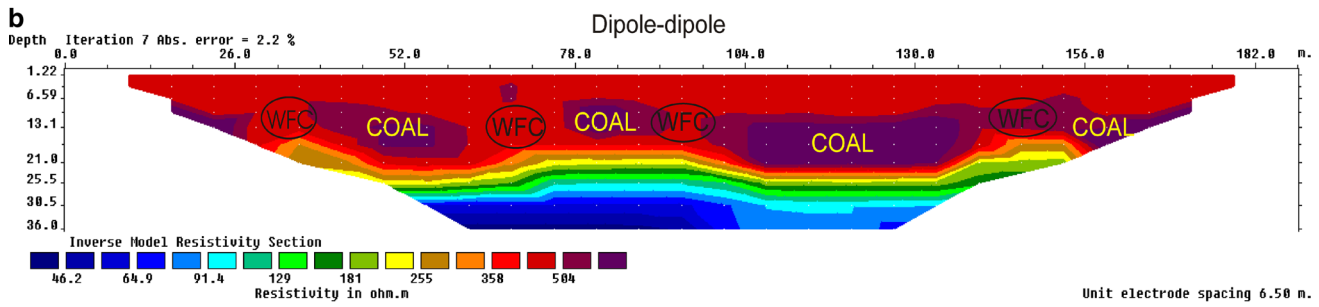
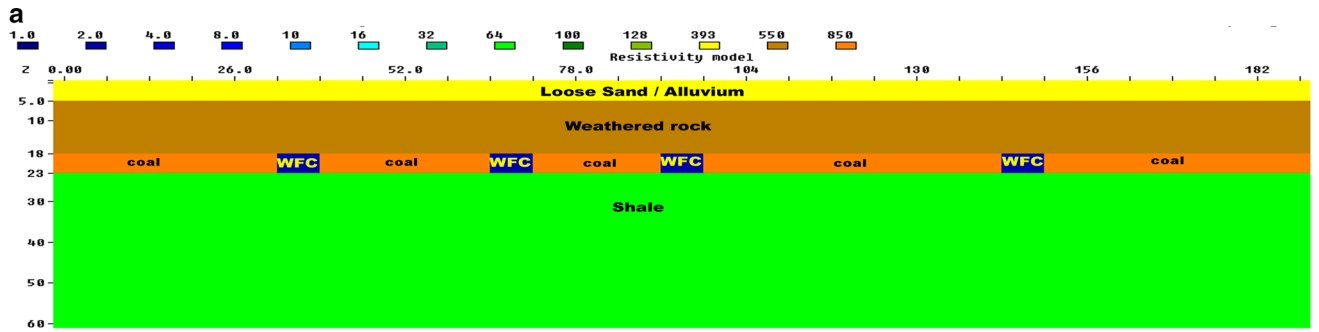
detection as: ground penetrating radar (GPR) and ERT (Leucci and De Giorgi 2005; El-Qady et al. 2005; Carbonel et al. 2013; Leucci 2006; Carpenter and Ekberg 2006; Lazzari et al. 2010); gravity and ERT (McGrath et al. 2002; Gambetta et al. 2011); ERT and seismic reflection tomography (SRT) (Cardarelli et al. 2010; Valois et al. 2010); microgravity (MG), GPR, ERT, Induced polarization (IP) (Brown et al. 2011); SRT and seismic Resonance, cross hole, ERT, gravity, magnetometry (M) and electromagnetic (EM) (McCann et al. 1987); EM, ERT, SRT (Bozzo et al. 1996); ERT and magnetometry (Gibson et al. 2004).

However, the imaging of subsurface cavities with various arrays has its own limitation and can produce different geoelectrical results. Wenner and Wenner–Schlumberger arrays have high vertical resolution, while dipole–dipole and pole–dipole arrays have high lateral resolution (Ward 1990). Stummer et al. (2004) suggested that combined data sets coming from different configurations carry more information than the individual data sets. de la Vega et al. (2003) suggested that combined inversion results have higher depth of investigation as well as lateral resolution compared to the inversion results obtained from each arrays separately. Later, Athanasiou et al. (2007) examined resistivity imaging data using combined weighed inversion for different array types. This study improves the interpretation in complex geological structures and produces a reliable geoelectrical model of subsurface.

There is no numerical study available on subsurface cavity detection considering board and pillar mining environment. In the present study, an attempt has been made to model numerically the resistivity response over water filled and air filled cavities associated old abandoned coal workings using ERI technique. Besides, joint inversion study was also undertaken considering Wenner–Schlumberger, dipole–dipole and pole–dipole electrode arrays.

Model simulation

In the absence of field resistivity data, the forward modelling approach is very useful to generate the resistivity response over subsurface cavities with water filled and air filled. Usually RES2DMOD software (Loke and Barker 1996a) has been used extensively to obtain apparent resistivity pseudo sections over synthetic models. This



software is based on the finite element method scheme which divides the subsurface into a number of rectangular meshes used to forward resistivity calculation. Four geological models have been simulated by assigning different resistivity values in rectangular mesh. A homogeneous near surface has been considered for every model. It has been assumed that cavities are fully air or water filled. Any air filled void space practically has an infinite resistivity. However, RES2DMOD software does not allow infinitive resistivity value. Therefore, a resistivity value 1,000,000 Ωm has been taken to simulate similar conditions. Water filled cavity resistivity is considered as 2 Ωm . The resistivity values for different formations have been assumed based on published literature (Palacky 1987). Variable pillar and galleries sizes have been considered for this numerical study in ordered to make the model more realistic. The exploited coal seam with pillars and galleries are simulated in the model considering presence and absence of coal barrier. These models were considered with using the concept given by Mohanty (2011). For every model, a multi electrode configuration of 30 equally spaced electrode with spacing 6.5 m has been applied. Figure 1a–c shows the geometry of three electrode configurations where AB and MN are current electrode separation (a) and potential electrode separation (a), respectively. K is the geometrical factor. Gaussian distributed random noise of 3 mV/A peak-to-peak amplitude has been added with the synthetic data for field environment simulation in order to make the models more realistic.

Model 1 (Fig. 2a) represents the geological model assuming a water filled cavity without a coal barrier. This model consists of four layered earth with different geological formations. The geological formations are loose sand/alluvium, weathered rock, coal seam (alternate pillars and galleries) and shale. The model dimensions are 186 m in length and 60 m in depth. Here, the gallery widths are kept constant as 6.5 m with variable pillars ranging from 19.5 m to 45.5 m. The resistivity values used for forward modelling is given in Table 1.

Model 2 (Fig. 3a) shows geological model water filled cavities with 1 m coal barrier as a roof over the working coal seam. The exploited coal seam has four cavities which are not equally spaced. The model length is 186 m and depth has been kept to 90 m, whereas cavity dimension has been kept 6.5 m in length and 4 m in width. Resistivity values used for forward modelling are given in Table 2.

Model 3 (Fig. 4a) represents the geological model identical to the model 1 except the galleries are replaced by air filled cavities. All other model parameters and geological formations have been kept identical as model 1. The

Table 1 Resistivity values of different layers of model 1

Model layers	Resistivity (Ωm)
Loose sand/alluvium	393
Weathered rock	550
Coal	850
Water filled cavity (WFC)	2
Shale	64

resistivity values used for forward modelling are given in Table 3.

Model 4 (Fig. 5a) shows in Fig. 4a consists of five layers including a thin barrier of 1 m above the exploited coal workings. The model dimensions are 186 m in length and 100 m in depth. The gallery widths are kept constant as 6.5 m with variable pillars width ranging from 32.5 m. The height of the coal working is kept at 4 m. Resistivity values used for the forward model are given in Table 4.

Later inversion procedure of apparent resistivity pseudo section has been conducted using RES2DINV software which is based on the smoothness-constrained least-squares method (deGroot-Hedlin and Constable 1990; Sasaki 1989; Loke et al. 2003).

Inversion of resistivity data

The inversion process has been computed using RES2DINV. It is based on smoothness constrained least-squares method (deGroot-Hedlin and Constable 1990; Sasaki 1992; Loke et al. 2003) which is based on the following Eq. (1):

$$(J^T + \lambda F)\Delta q_k = J^T g - \lambda F q_k \quad (1)$$

$$F = \alpha_X C_X^T C_X + \alpha_Z C_Z^T C_X$$

C_X and C_Z are horizontal and vertical roughness filters, J is Jacobean matrix of partial derivatives, J^T is the transpose of J , λ is damping factor, q is model change vector, g is data misfit vector, α_X and α_Z are relative weights given to the smoothness filter in X and Z direction, q is model resistivity values, k is the number of iteration, Δq_k is the change in model parameter for k th iteration.

Loke et al. (2003) used cell based inversion technique for adequately model complex structures with an arbitrary resistivity distribution. The 2D model implemented in this software divides the subsurface into rectangular blocks

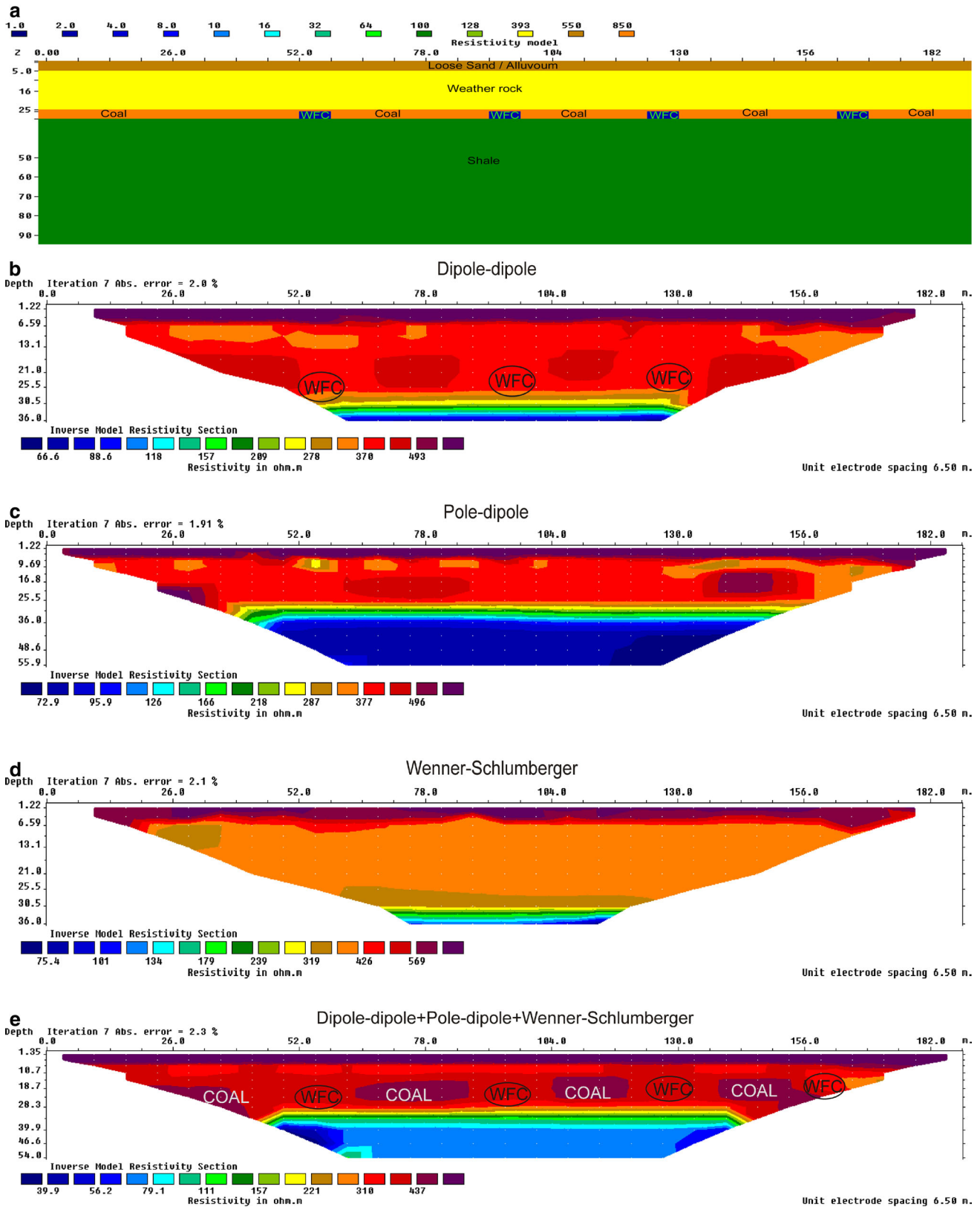


Fig. 3 Inversion results: **a** Resistivity model 2 employed; **b** inverted section using dipole–dipole array; **c** inverted section using pole–dipole array; **d** inverted section using Wenner–Schlumberger array;

e jointly inverted section using dipole–dipole, pole–dipole and Wenner–Schlumberger array

Table 2 Resistivity values of different layers of model 2

Model layer	Resistivity (Ωm)
Loose sand/alluvium	550
Weathered rock	393
Coal	850
Shale	100
Water filled cavity (WFC)	2

whose positions and sizes are fixed (Loke et al. 2003) and the resistivity of each block are modified in an iterative manner to minimize the difference between measured and calculated apparent resistivity values. The approach as used by Sasaki (1992) and Loke et al. (2003) have been used where the widths of the blocks are set at half the spacing between adjacent electrodes. This method gives better result in case of smooth variation of subsurface geology (Loke and Barker 1996b).

Results

Four geoelectrical models were considered assigning for resistivity imaging study using inversion of arrays separately and joint inversion approach.

Model 1

Figure 2b, c, d represent inverted resistivity sections over model 1 corresponding to dipole–dipole, pole–dipole and Wenner–Schlumberger electrode array respectively. It is evident that dipole–dipole and pole–dipole inverted resistivity section clearly bring out the water filled cavities in comparison to inverted section corresponding to Wenner–Schlumberger. This might be due to poor lateral resolution of Wenner–Schlumberger array. The dipole–dipole inverted resistivity section (Fig. 2b) clearly imaged four subsurface cavities due to strong resistivity contrast exist in the lateral direction. Resistivity values greater than 504 Ωm indicates presence of coal pillars, whereas low resistivity value around 358–504 Ωm indicates galleries with water-logged. But pillars and galleries are not properly delineated. Figure 2c approached close to the target depth corresponding to top of water filled cavity. Here, high resistivity value greater than 440 Ωm corresponds to coal pillars and low resistivity values nearly about 440 Ωm indicates water filled galleries. Figure 2d represents the low resistivity values of 211 Ωm against galleries and high resistivity value of 500–668 Ωm against coal pillars. In

order to improve the interpretation, joint inversion has been carried out using all the three arrays. Joint inverted resistivity section is shown in Fig. 2e. In this inverted section, galleries as well as pillars have been image very clearly. Low resistivity value of 328 Ωm corresponds to galleries and high resistivity 519 Ωm indicates the coal pillars.

Model 2

Figure 3b, c, d illustrates inverted resistivity sections corresponding to dipole–dipole, pole–dipole and Wenner–Schlumberger electrode array respectively for water filled cavities with coal barrier. Only dipole–dipole array could able to identify three water filled cavity and coal pillars individually where as other two arrays was could not detect the cavities. In Fig. 3b, low resistivity value of 300–370 Ωm zone at depth between 15 and 25 m due to water filled cavity and high resistivity value of 370–430 Ωm indicates the presence of coal pillars. Subsequently, three array data was jointly inverted which was shown in Fig. 3e and it succeed to delineate water filled cavity very clearly in presence of coal barrier and coal pillars. High resistivity (437 Ωm) area indicates coal pillars and high resistivity value of 310–370 Ωm areas indicates water filled galleries. Here three cavities are very clear and the forth one (located at 165 m) is at the edge of the inversion area.

Model 3

Figure 4b, c, d illustrates inverted resistivity sections over model 3 corresponding to dipole–dipole, pole–dipole and Wenner–Schlumberger array, respectively. It is observed that the pole–dipole inverted section clearly bring out three air filled cavities with large resistivity value in comparison with section for dipole–dipole and Wenner–Schlumberger array. In Fig. 4b, the high resistivity value greater than 619 Ωm corresponds to air filled cavities whereas the coal pillars corresponding to low resistivity values in the range of 544–619 Ωm . In this section, galleries and coal pillars were not delineated properly. Inverted resistivity section for pole–dipole array was shown in Fig. 4c. Like earlier model it also indicates high resistivity value of 616 Ωm against galleries and low reactivity value of 544–616 Ωm against solid coal galleries. Figure 4d corresponding to Wenner–Schlumberger array failed to delineate void and coal pillars. But only a high resistive area has been observed. The joint inverted section shown in Fig. 4d has significantly improved the result. Here all four galleries with resistivity value of 584 Ωm and pillars with resistivity

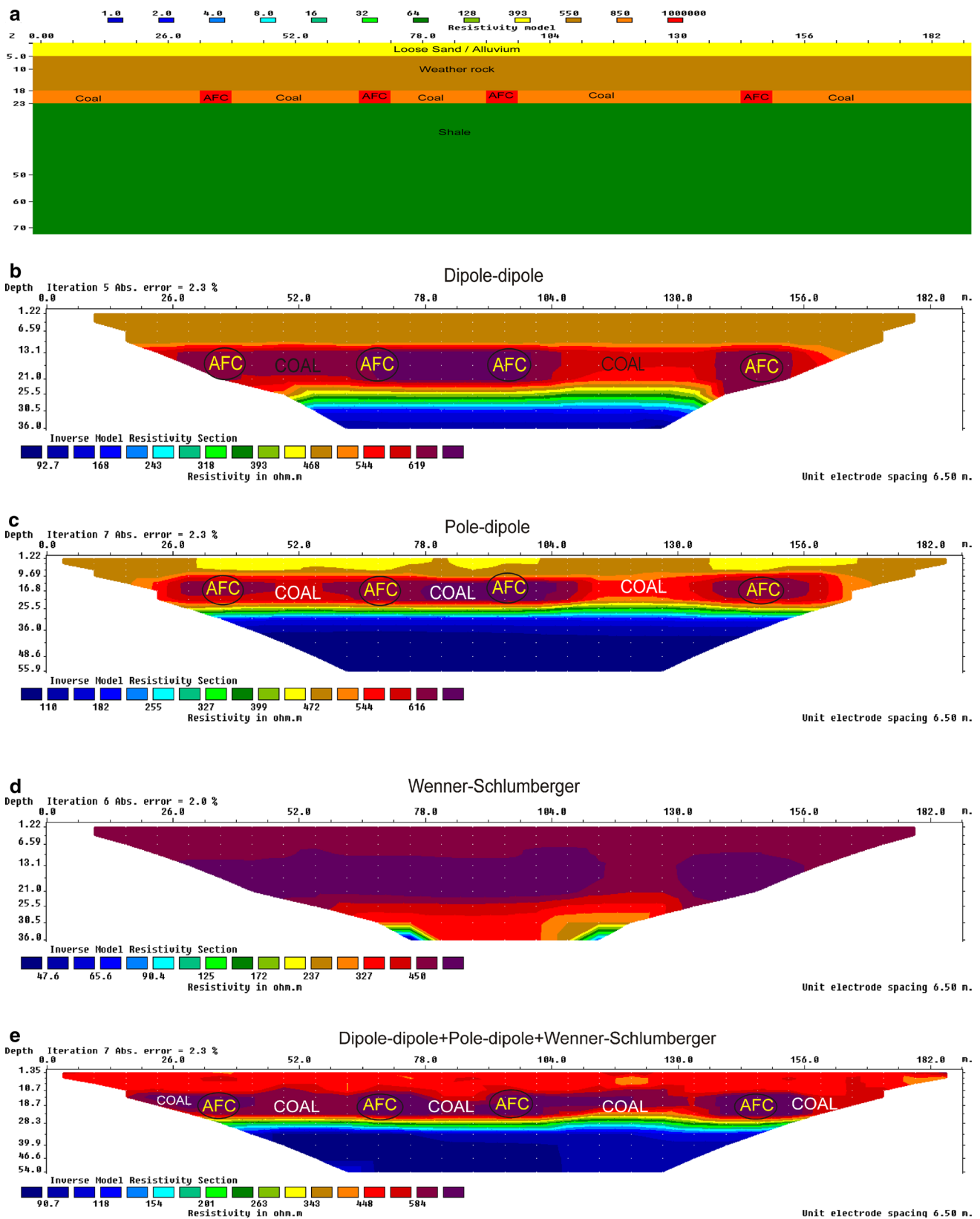


Fig. 4 Inversion results: **a** Resistivity model 3 employed; **b** inverted section using dipole–dipole array; **c** inverted section using pole–dipole array; **d** inverted section using Wenner–Schlumberger array;

e jointly inverted section using dipole–dipole, pole–dipole and Wenner–Schlumberger array

Table 3 Resistivity values of different layers of model 3

Model layer	Resistivity (Ωm)
Loose sand/alluvium	393
Weathered rock	550
Coal	850
Shale	64
Air filled cavity (AFC)	1,000,000

values of 584 Ωm were delineated very clearly in comparison to other three inverted section separately.

Model 4

Figure 5b, c, d indicates the inverted resistivity section over model 4 for dipole–dipole, pole–dipole and Wenner–Schlumberger electrode array. Here, all the three array have been unbaled to provide any significant resistivity response over air filled cavity in presence of coal barrier. This might be due to the presence of high resistive coal barrier above the exploited section which prevents cavity detection. Figure 5e presents joint inverted model section of all three array and able to produce a better image over the cavities. High resistivity values of 417–715 Ωm indicate air filled cavities and low resistivity value of 290–417 Ωm indicate solid coal pillars.

Table 5 shows the differences and quantifying errors between various electrode configurations for above four models.

Maillol et al. (1999) suggested that it is impossible to delineate empty galleries as high resistivity coal seam prevent an adequate detection and only possible hint of the presence of a void is the generally maximum values of resistivity. However, the joint inversion allows us to detect empty galleries with and without coal barrier.

Mohanty (2011) showed that air filled cavities with and without coal barrier can be detected and delineated clearly using seismic reflection method. In case of water filled cavities with a coal barrier this method did not work to detect and delineate targets, whereas water filled cavities without a coal barrier can be detected with a poor signature. The joint inversion of electrode arrays is a superior technique to detect water or air filled cavities with or without a coal barrier. The present study shows that the joint inversion of different electrode arrays may be useful when seismic reflection method failed to provide significant response.

Conclusions

The following conclusions are arrived from the present study

1. The inverted resistivity section for pole–dipole electrode array corresponding to water filled cavity without barrier (model 1) detected four cavities, whereas dipole–dipole and Schlumberger array could detect three out of four water filled cavities. When all the three arrays are jointly inverted, the result improved significantly with detection and delineation of all four water filled cavities.
2. In case of model 2, the inverted resistivity section corresponding to the result from dipole–dipole array provides only three water filled cavities with a coal barrier, whereas pole–dipole and Schlumberger arrays type could not detect any of the cavities. When all the three array data are jointly inverted, the resistivity section clearly brings out all three cavities and the fourth one (located at 165 m) is at the edge of the inversion.
3. Similar study has been undertaken by replacing water filled cavities with air filled cavities in model 3. The inverted result for model 3 using dipole–dipole, pole–dipole and Wenner–Schlumberger array was unable to distinguish subsurface cavities. However, a high resistive layer was detected which may be the overall response of air filled cavities, whereas the jointly inverted section for these three arrays significantly improved the result with detection and delineation of four air filled cavities.
4. Finally, the inverted resistivity section was generated considering air filled cavities with barrier in model 4. The inverted sections of three arrays were unable to detect air filled cavities in the presence of a coal barrier, whereas, the jointly inverted resistivity section for three arrays was able to delineate four cavities clearly.
5. It is observed that the inverted resistivity section (for model 2, 3, 4) against single array could not produce meaningful interpretation due to its limitation. However, when it is jointly inverted, the inverted resistivity section improves the interpretation significantly in detecting four cavities with or without a barrier. This might be due to joint inversion of arrays with various properties. In this approach, it combines dipole–dipole and pole–dipole arrays which are very sensitive to horizontal variation and Wenner–Schlumberger which

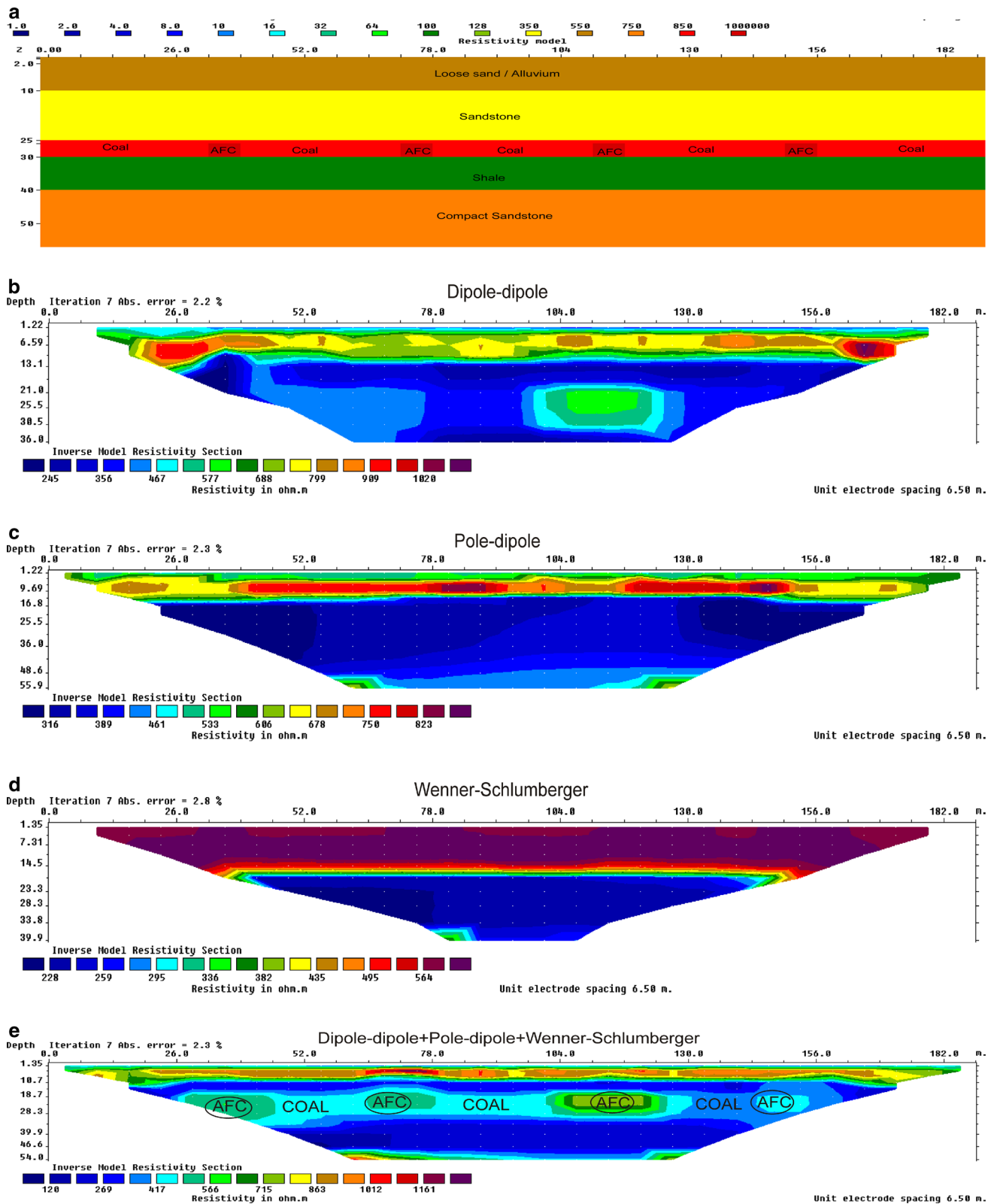


Fig. 5 Inversion results: **a** Resistivity model 4 employed; **b** inverted section using dipole-dipole array; **c** inverted section using pole-dipole array; **d** inverted section using Wenner-Schlumberger array;

e jointly inverted section using dipole-dipole, pole-dipole and Wenner-Schlumberger array

Table 4 Resistivity values of different layers of model 4

Model layer	Resistivity (Ωm)
Loose sand/alluvium	550
Sandstone	350
Coal	850
Shale	100
Compact sandstone	750
Air Filled Cavity (AFC)	1,000,000

Table 5 Differences and quantifying errors between various electrode configurations for four models

Model no	ERT array	Maximal depth of penetration (m)	RMS error (%)	The number of the iteration	Target (cavity detected)
Model 1	Dipole–dipole	36.8	2.2	7	4
	Pole–dipole	55.9	2.2	7	4
	Wenner–Schlumberger	36.0	2.1	7	4
	Jointly	54.8	2.4	7	4
Model 2	Dipole–dipole	36.0	2.0	7	4
	Pole–dipole	55.9	1.91	7	None
	Wenner–Schlumberger	36.8	2.1	7	None
	Jointly	54.8	2.3	7	4
Model 3	Dipole–dipole	36.8	2.3	5	Not clearly
	Pole–dipole	55.9	2.3	7	3
	Wenner–Schlumberger	36.8	2.0	6	None
	Jointly	54.8	2.3	7	4
Model 4	Dipole–dipole	36.8	2.2	7	None
	Pole–dipole	55.9	2.3	7	None
	Wenner–Schlumberger	36.8	2.5	5	None
	Jointly	54.8	2.3	7	4

is very sensitive to vertical variation in the subsurface resistivity.

6. Finally, it can be concluded that joint inversion is a very useful technique for a better subsurface image in case of complex geological condition. Also, it can be noted that this approach is an important part for planning of deeper coal seam mining under cavity zone and stabilized the surface.

Acknowledgments The authors are thankful to Department of Science and Technology (Project SR/S4/ES-656/2013), Government of India for supporting of this research work.

References

- Athanasiou EN, Tsourlos PI, Papazachos CB, Tsokas GN (2007) Combined weighted inversion of electrical resistivity data arising from different array types. *J Appl Geophys* 62:124–140. doi:10.1016/j.jappgeo.2006.09.003
- Bauman P (2005) 2-D resistivity surveying for hydrocarbons—a primer. *CSEG Rec* 30:25–33
- Bondarenko VM, Victorow GG, Demin NV, Kulkov BN, Lumpov EE, Christich VA (1983) *New methods in engineering geophysics*. Nedra, Moscow
- Bozzo E, Lombardo S, Merlanti F (1996) Geophysical studies applied to near-surface karst structures: the dolines. *Ann Geophys* XXXIX 1:23–38
- Brown WA, Stafford KW, Shaw FM, Grubbs A (2011) A comparative integrated geophysical study of Horseshoe Chimney Cave, Colorado Bend State Park, Texas. *Int J Speleol* 40(1):9–16
- Carbonel D, Gutiérrez F, Linares R, Roqué C, Zarroca M, McCaLpin J, Guerrero J, Rodriguez V (2013) Differentiating between gravitational and tectonic faults by means of geomorphological mapping, trenching and geophysical surveys: the case of Zenzano Fault (Iberian Chain, N Spain). *Geomorphology* 189:93–108. doi:10.1002/ESP.3440
- Cardarelli E, Cercato M, Cerreto A, Di Filippo G (2010) Electrical resistivity and seismic refraction tomography to detect buried cavities. *Geophys Prospect* 58:685–695
- Carpenter PJ, Ekberg DW (2006) Identification of buried sinkholes, fractures and soil pipes using ground-penetrating radar and 2D electrical resistivity tomography. *Proceedings of the Highway Geophysics—NDE Conference*, pp 437–449
- Chalikakis K, Plagnes V, Guerin R, Bosch F, Valois R (2011) Contribution of geophysical methods to karst-system

- exploration: an overview. *Hydrogeol J* 19(6):1169–1180. doi:[10.1007/s10040-011-0746-x](https://doi.org/10.1007/s10040-011-0746-x)
- Chambers JC, Kuras O, Meldrum PI, Ogilvy RD, Hollands J (2006) Electrical resistivity tomography applied to geologic, hydrogeologic, and engineering investigations at a former waste-disposal site. *Geophysics* 71(6):B231–B239
- Cigna AA (2005) Radon in caves. *Int J Speleol* 34(1–2):1–18. Bologna (Italy). ISSN 0392-6672
- Clark F (2002) The problem of radon in caving: Education, education and science Environmental radon newsletter. Department of geology, Oxford Brookes University
- Colella A, Lapenna V, Rizzo E (2004) High-resolution imaging of the High Agri Valley Basin (Southern Italy) with electrical resistivity tomography. *Tectonophysics* 386:29–40. doi:[10.1016/j.tecto.2004.03.017](https://doi.org/10.1016/j.tecto.2004.03.017)
- Dahlin T, Zhou B (2004) A numerical comparison of 2D resistivity imaging with 10 electrode arrays. *Geophys Prospect* 52:379–398. doi:[10.1111/j.1365-2478.2004.00423.x](https://doi.org/10.1111/j.1365-2478.2004.00423.x)
- de la Vega M, Osella A, Lascano E (2003) Joint inversion of Wenner and dipole–dipole data to study a gasoline-contaminated soil. *J Appl Geophys* 54:97–109
- deGroot-Hedlin C, Constable SC (1990) Occam’s inversion to generate smooth, two dimensional models from magnetotelluric data. *Geophysics* 55:1613–1624
- El-Qady G, Hafez M, Abdalla MA, Ushijima K (2005) Imaging subsurface cavities using geoelectric tomography and ground-penetrating radar. *J Cave Karst Stud* 67(3):174–181
- Evangelos CG, Yannis CM, Christos PP, Evangelos KK (2015) Large scale electrical resistivity tomography survey correlated to hydrogeological data for mapping groundwater salinization: a case study from a multilayered coastal aquifer in Rhodope, Northeastern Greece. *J Environ Process*. doi:[10.1007/s40710-015-0061-y](https://doi.org/10.1007/s40710-015-0061-y)
- Gambetta M, Armadillo E, Carmisciano C, Stefanelli P, Cocchi L, Tontini FC (2011) Determining geophysical properties of a near surface cave through integrated microgravity vertical gradient and electrical resistivity tomography measurements. *J Cave Karst Stud* 73(1):11–15
- Gibson PJ, Lyle P, George DM (2004) Application of resistivity and magnetometry geophysical techniques for near-surface investigations in karstic terranes in Ireland. *J Cave Karst Studies* 66(2):35–38
- Gillmore GK, Sperrin M, Philips P, Denman A (1999) Radon hazard, geology and exposure of cave users: a case study and some theoretical perspectives. *Environ Int* 22:S409–S413
- Griffiths DH, Barker RD (1993) Two-dimensional resistivity imaging and modelling in areas of complex geology. *J Appl Geophys* 29:211–226. doi:[10.1016/0926-9851\(93\)90005-J](https://doi.org/10.1016/0926-9851(93)90005-J)
- Hakl J, Hunyadi I, Csige I, Geczy G, Lenart I, Varhegy A (1997) Radon transport phenomena studied in Karst Caves-international experiences on radon levels and exposures. *Radiat Meas* 28(1–6):675–684
- Hallof PG (1966) The use of resistivity results to outline sedimentary rocks types in Ireland. *Min Geophys, SEG*
- Hutchinson DJ, Phillips C, Cascante G (2002) Risk considerations for crown pillar stability assessment for mine closure planning. *J Geotech Geol Eng* 20:41–64
- Jain SC, Kumar R, Roy A (1973) Some results of experimental geophysical surveys for location of ancient gold workings, Kolar, India. *Geophys Prospect* 21:229–242
- Johnson WJ, Snow RE, Clark JC (2002) Surface geophysical methods for detection of underground mine working. Abstract of Symposium on Geotechnical Methods for Mine Mapping Verifications, Charleston, West Virginia, 29 October 2002
- Jovanovic P (1996) Radon measurement in karst Caves in Slovenia. *Environ Intern* 22(suppl 1):S429–S432
- Lazzari M, Loperte A, Perrone A (2010) Near surface geophysics techniques and geomorphological approach to reconstruct the hazard cave map in historical and urban areas. *Adv Geosci* 24:35–44
- Legault JM, Carriere D, Petrie L (2008) Synthetic model testing and distributed acquisition dc resistivity results over an unconformity uranium target from the Athabasca Basin, northern Saskatchewan. *Lead Edge* 27(1):46–51
- Leucci G (2006) Contribution of ground penetrating radar and electrical resistivity tomography to identify the cavity and fractures under the main church in Botrugno (Lecce, Italy). *J Archaeol Sci* 33:1194–1204
- Leucci G, De Giorgi L (2005) Integrated geophysical surveys to assess the structural conditions of a karstic cave of archaeological importance. *Nat Hazards Earth Syst Sci* 5:17–22
- Logn O (1954) Mapping nearly vertical discontinuities by earth resistivities. *Geophysics* 19:739–760
- Loke MH, Barker RD (1996a) Rapid least-squares inversion of apparent resistivity pseudosections by a quasi-Newton method. *Geophys Prospect* 44:131–152. doi:[10.1111/j.1365-2478.1996.tb00142.x](https://doi.org/10.1111/j.1365-2478.1996.tb00142.x)
- Loke MH, Barker RD (1996b) Practical techniques for 3D resistivity surveys and data inversion1. *Geophys Prospect* 44:499–523
- Loke MH, Acworth I, Dahlin T (2003) A comparison of smooth and blocky inversion methods in 2D electrical imaging surveys. *Explor Geophys* 34:182–187
- Maillet GM, Rizzo E, Revil A, Vella C (2005) High resolution electrical resistivity tomography (ERT) in a transition zone environment: application for detailed internal architecture and infilling processes study of a Rhône River paleo-channel. *Mar Geophys Res* 6:317–328. doi:[10.1007/s11001-005-3726-5](https://doi.org/10.1007/s11001-005-3726-5)
- Maillol JM, Seguin MK, Gupta OP, Akhauri HM, Sen N (1999) Electrical resistivity tomography survey for delineating uncharted mine galleries in West Bengal, India. *Geophys Prospect* 47:103–116. doi:[10.1046/j.1365-2478.1999.00126.x](https://doi.org/10.1046/j.1365-2478.1999.00126.x)
- Martinez J, Benavente J, García-Aróstegui JL, Hidalgo MC, Rey J (2009) Contribution of electrical resistivity tomography to the study of detrital aquifers affected by seawater intrusion-extrusion effects: the river Vélez delta (Vélez-Málaga, southern Spain). *Eng Geol* 108:161–198. doi:[10.1016/j.enggeo.2009.07.004](https://doi.org/10.1016/j.enggeo.2009.07.004)
- McCann DM, Jackson PD, Culshaw MG (1987) The use of geophysical surveying methods in the detection of natural cavities and mineshafts. *Q J Eng Geol* 20:59–73
- McGrath RJ, Styles P, Thomas E, Neale S (2002) Integrated high resolution geophysical investigations as potential tools for water resource investigations in karst terrain. *Environ Geol* 42:552–557
- Mohanty PR (2011) Numerical modeling of P-waves for shallow subsurface cavities associated with old abandoned coal workings. *J Environ Eng Geophys* 16:165–175. doi:[10.2113/JEEG16.4.165](https://doi.org/10.2113/JEEG16.4.165)
- Ntwaeaborwa ON, Kgwadi ND, Taole SH, Strydom R (2004) Measurement of the equilibrium factor between radon and its progeny in the underground mining environment. *Health Phys* 86(4):374–377
- Palacky GJ (1987) Resistivity characteristics of geologic targets. In: Nabighian MN (ed) *Electromagnetic methods in applied geophysics*, vol 1, SEG Investigations in Geophysics Series No. 3
- Reynolds JM (1997) *An introduction to applied and environmental geophysics*. John Wiley & Sons, Chichester, p 796
- Riddle G (2012) Detection of clandestine tunnels using seismic refraction and electrical resistivity tomography. PhD dissertation, University of Alberta
- Rucker D, Loke MH, Levitt MT, Noonan GE (2010) Electrical resistivity characterization of an industrial site using long electrodes. *Geophysics* 75(4):WA95–WA104

- Sasaki Y (1989) Two-dimensional joint inversion of magnetotelluric and dipole-dipole resistivity data. *Geophysics* 54:174–187
- Sasaki Y (1992) Resolution of resistivity tomography inferred from numerical SIMULATION1. *Geophys Prospect* 40:453–463
- Singh J, Jha BP (1972) Resistivity profiles over some dykes of Dhanbad. *Geophys Prospect* 20:130–141
- Stanley WD, Jackson DB, Zohdy AAR (1976) Deep electrical investigation in the Long Valley geothermal area, California. *J Geophys Res* 81:810–820
- Stummer P, Maurer H, Green A (2004) Experimental design. Electrical resistivity data sets that provide optimum subsurface information. *Geophysics* 69(1):120–139
- Thomas B, Roth MJS (1999) Evaluation of site characterization methods for sinkholes in Pennsylvania and New Jersey. *Eng Geol* 52:147–152
- Tsokas GN, Tsourlos PI, Vargemezis G, Novack M (2008) Non-destructive electrical resistivity tomography for indoor investigation: the case of Kapnikarea church in Athens. *Archaeol Prospect* 15(1):47–61
- Valois R, Bermejo L, Guérin R, Hinguant S, Pigeaud R, Rodet J (2010) Karstic morphologies identified with geophysics around Saulges caves (Mayenne, France). *Archaeol Prospect* 17:151–160
- Van SM (2002) Detection of sinkholes using 2D electrical resistivity imaging. *J Appl Geophys* 50:393–399. doi:10.1016/S0926-9851(02)00166-0
- Van NR, Cook KL (1966) Interpretation of resistivity data, USCGS Professional Paper-499, US Govt. Printing Office, Washington
- Ward S (1990) Resistivity and induced polarization methods. *Geotech Environ Geophys* 1:147–189
- Wilson SR, Ingham M, McConchie JA (2006) The applicability of earth resistivity methods for saline interface definition. *J Hydrol* 316(1–4):301–312
- Zarroca M, Bach J, Linares R, Pellicer XM (2011) Electrical methods (VES and ERT) for identifying, mapping and monitoring different saline domains in a coastal plain region (Alt Empordà, Northern Spain). *J Hydrol* 409(1–2):407–422. doi:10.1016/j.jhydrol.2011.08.052
- Zarroca M, Linares R, Bach J, Roque C, Moreno V, Font LI, Baixeras C (2012) Integrated geophysics and soil gas profiles as a tool to characterize active faults: the Amer fault example (Pyrenees, NE Spain). *Environ Earth Sci* 67:889–910. doi:10.1007/s12665-012-1537-y
- Zhou W, Beck BF, Stephenson JB (2000) Reliability of dipole-dipole electrical resistivity tomography for defining depth to bedrock in covered karst terranes. *Environ Geol* 39:760–766. doi:10.1007/s002540050491
- Zohdy AAR (1969) The use of Schlumberger and equatorial soundings in groundwater investigations near El Paso, Texas. *Geophysics* 34:713–728
- Zohdy AAR, Anderson LA, Muffler LJP (1973) Resistivity, self-potential and induced polarisation surveys of a vapour dominated geothermal system. *Geophysics* 38:1130–1144